A Markovian Design of Bi-Directional Robust Header Compression for Efficient Packet Delivery in Wireless Networks

Wenhao Wu, *Member, IEEE*, and Zhi Ding, *Fellow, IEEE*

***Abstract*— As a major tool for improving transport efficiency by reducing header redundancy, robust header compression (ROHC) plays an important role in modern packet-switched wireless networks. However, widespread ROHC deployment is in sharp contrast to extremely limited number of research works on ROHC analysis and design optimization. In this paper, we investigate a novel trans-layer approach in designing a bi-directional ROHC under unreliable wireless channel conditions. We propose a novel ROHC compressor design based on a new formulation in terms of a partially observable Markov decision process (POMDP). This new formulation robustly explores the lower protocol layer signaling to optimize the compressor actions dynamically on the header level and feedback polling. Our design approach improves the transmission efficiency and curtails the required ROHC feedback overhead. Furthermore, to reduce the complexity of our optimized POMDP design, we propose a low-complexity suboptimal ROHC compressor. Our novel trans-layer designs achieve more flexible trade-offs between transmission efficiency and feedback overhead than existing ROHC compressors. They also demonstrate a substantial performance improvement under poor channel conditions and long feedback delay.**

***Index Terms*— Packet networks, packet header, compression, ROHC, decision process, partial observation.**

I. Introduction

IN MIGRATING from 3G to 4G and now onto 5G services, the wireless network infrastructure continues to converge towards an all-Internet Protocol (IP) packet-switched (PS) architecture for most wireless services [1, Ch. 4.5], [2]. At the same time, the explosive growth of wireless data traffics and services underlines the acute need to continuously enhance the network efficiency under bandwidth and other practical resource constraints. It is evident that future improvement of wireless network performance should not focus only on MAC and PHY layer techniques. Instead, closer examining the IP-based protocol stacks over wireless infrastructures from a trans-layer perspective may reveal untapped potentials for significant performance improvement largely neglected by most existing research works.

Manuscript received August 9, 2017; revised August 16, 2018; accepted October 1, 2018. Date of publication October 18, 2018; date of current version January 8, 2019. This work was supported in part by the National Science Foundation under Grant 1702752 and Grant 1824553. The associate editor coordinating the review of this paper and approving it for publication was R. Zheng. *(Corresponding author: Wenhao Wu.)*

The authors are with the Department of Electrical and Computer Engineering, University of California at Davis, Davis, CA 95616 USA (e-mail: wnhwu@ucdavis.edu; zding@ucdavis.edu).

Color versions of one or more of the figures in this paper are available online at http://ieeexplore.ieee.org.

Digital Object Identifier 10.1109/TWC.2018.2875448

Because of the large header size relative to the corresponding payload size of many data packets, RObust Header Compression (ROHC) has been utilized as an important process to improve wireless transmission-efficiency in IP-based networks. For many applications such as VoIP, interactive media, sensor networks, and Internet-of-Things (IoT), the size of headers are usually comparable to or sometimes even larger than that of the packet payload, leading to severe under-utilization of limited radio resources. ROHC techniques leverage the fact that packets which belong to the same service stream in a radio bearer [3] typically have headers with high redundancy for compression. In fact, many header fields such as source and destination addresses may remain static, or may vary non-abruptly (e.g. sequence number) throughout the lifetime of the data flow. Typically residing between the internet IP/UDP/RTP layers and wireless RLC/MAC/PHY layers, ROHC is responsible for curtailing header redundancy that could otherwise severely waste the network connection rate achievable by PHY/MAC layers. ROHC is specifically designed for wireless links with larger packet error rate (PER) and longer round trip time (RTT) than wired links, in order to balance between compression efficiency and robustness against poor channel conditions. To date, ROHC has been standardized for various header profiles [4]–[6] and has found widespread applications in many scenarios including the 4G-LTE cellular network [3], satellite links [7], [8], underwater acoustic networks [9], [10], and tactical edge networks [11]. In light of the rapid growth of IoT, whose data link layer is often characterized by limited packet size and high PER, it is foreseeable that ROHC will play an even greater role in the near future as a key enabling technology to achieve high efficiency [12], [13].

Although ROHC has been widely deployed in various modern wireless communication systems, it is surprising that thus far it has only attracted scant research attention. Most existing ROHC studies centered on simulation-based performance evaluations, which are highly dependent on the chosen system settings and simulation environments, and naturally lead to empirical ROHC parameter tuning [14]–[22]. In fact, existing attempts to rigorously model, analyze, and optimize these ROHC mechanisms have been very limited. The pioneering work of [23] proposed a comprehensive analytical framework composed of 4 processes, including the packet source, the channel, the compressor and the decompressor. These 4 processes are modeled as either deterministic finite-state machine (FSM) or Markov process interacting with

one another. Based on this framework, performances in terms of compression efficiency, robustness and transparency are analyzed. An optimization problem to maximize the efficiency under the transparency constraint with respect to the header encoding parameters is studied. The analytical framework in [24] has no packet source and introduced a compressor process with slow start and periodic refreshment. The robustness of ROHC versus the header encoding parameters are studied under this framework. Reference [25] proposed an even simpler analytical model with only the decompressor FSM and a memoryless channel, and focused on the impact of header encoding parameters on robustness and efficiency. Reference [26] adopted a random memoryless compressor model and a Markov channel model to study the behavior of ROHC for different packet flow profiles. These works all investigate the simple uni-directional ROHC where there is no feedback to help the compressor to adjust the header compression level.

One common shortcoming among existing ROHC standards and most related studies is to isolatedly investigate ROHC within a single layer in the protocol stack. Despite the fact that ROHC is designed specifically for wireless packet-switched links, there have been few attempts thus far to leverage trans-layer network information in ROHC design and optimization. We stress that trans-layer network information is available from other layers within the network protocol that can help boost the performance of the ROHC compressor/decompressor at little or no additional cost. For instance, the authors of [27] proposed to examine the hybrid ARQ feedbacks from MAC layer to infer the success or the failure of packet header recovery without relying on other dedicated feedback. Nevertheless, this work requires the less practical assumption of error-free and zero-delay (near instantaneous) "trans-layer information" for such inference. Exploiting this trans-layer design philosophy, our recent work [28] proposed a novel control framework for uni-directional ROHC based on partially observable Markov decision process (POMDP) without any ROHC feedback channel. This newly proposed ROHC framework demonstrates significant performance gains over conventional, timer-based ROHC control even if the trans-layer information does exhibit moderate error probabilities and non-zero delays. Note that POMDP is a control optimization strategy that has found application in many fields [29], [30] including in wireless communication systems [31]–[36]. We have also studied the optimization of ROHC and user grouping for Multimedia Broadcast Multicast Service (MBMS) in [37] and [38].

Encouraged by these preliminary successes, in the present work we study the trans-layer control framework for the more general bi-directional ROHC. Different from the uni-directional ROHC [28], bi-directional ROHC decompressor can send limited feedbacks about the decompressor's state on a designated reverse channel to assist the compressor's control of its compression level dynamically. One motivation to exploit ROHC feedback is that our previous uni-directional ROHC design requires additional APIs from other layers, which may not be readily available in practice. In contrast, the dedicated ROHC feedback is confined to one layer only is thus more implementation-wise friendly. Although the presence of a feedback channel appears to simplify the design of control logic in the ROHC compressor, in many practical scenarios with limited feedback resources, however, one must assess the trade-off between compression efficiency and feedback overhead. In other words, frequent feedbacks from the decompressor would improve the header compression efficiency by providing timely knowledge of the decompressor state. However, the improvement requires more feedback channel resource and can be quite costly.

Considering the performance-resource trade-off in this work, we develop a polling-based (on-demand) decompressor feedback mechanism for the bi-directional ROHC. In this novel design, decompressor feedback is transmitted only when polled by the compressor upon determining that its local trans-layer information alone is insufficient for it to confidently control its header compression decision. Specifically, our design framework proposes to complementarily exploit both the ROHC feedback and trans-layer information. In this new framework, the decisions at the compressor are two-fold, with respect to (w.r.t.) the compression level and when to send a polling message for decompressor feedback based on the compressor's confidence on the decompressor state. We formulate the optimal control process as a new POMDP paradigm to achieve a flexible trade-off between feedback rate and transmission efficiency. Compared with our previous work [28], however, the introduction of the polling action and a header source model leads to a much larger state space, such that the rigorous POMDP formulation becomes vulnerable to the "curse of dimensionality" problem as the delay of the trans-layer information and ROHC feedback increases. To effectively mitigate the resulting high computation complexity, we propose a suboptimal myopic control strategy based on a belief update process without having to fully solve the POMDP instance with complexity that grows exponentially with the feedback delay. Our test results show that both design schemes achieve better trade-off than conventional bi-directional ROHC design, thereby enabling practical implementation at much worse channel conditions and for longer feedback delays.

We organize the manuscript as follows. Section II describes the principle and the key components of the ROHC mechanism and specifies the underlying channel model used in this work. Section III presents the POMDP design framework for our trans-layer ROHC compressor. In Section IV, we provide a detailed complexity analysis for the POMDP formulation and develop a low-complexity trans-layer compressor design for broader and more practical applications. Section V presents some numerical results before the final conclusions of Section VI.

II. System Model

A. Notations

We use regular font, bold lower-case, bold upper-case, and calligraphic letters, respectively, to denote scalars, vectors, matrices, and sets. Let $\{\mathbf{A}\}_{ij}$ and $\{\mathbf{a}\}_i$, respectively, be the (i,j)-th entry of $\mathbf{A}$ and the i-th entry of $\mathbf{a}$. Let $\mathcal{A}\times\mathcal{B}$ denote Cartesian product of sets $\mathcal{A}$ and $\mathcal{B}$. The subscript $(\cdot)^T$ indicates matrix transpose. We define an indicator function $\mathbf{1}[expr]=1$

if logical expression "*expr*" is true and $\mathbf{1}[expr] = 0$ otherwise. We let the time index of the packet session be denoted by "$[t]$" which represents the t-th packet transmitted. All indexing variables start from 0 to be consistent with the popular C programming convention. We also use "$\wedge$" and "$\vee$" to denote logical AND and logical OR, respectively.

B. Basics of ROHC

Since ROHC is a part of wireless networks not well known to many readers, we shall provide a short introduction. ROHC is typically the interface between two different packet protocols. Taking 4G LTE as an example, the ROHC mechanism resides in the Packet Data Convergence Protocol (PDCP) sublayer which connects the global IP infrastructure and (the Radio Link Control sublayer of) the cellular network. A key function of the PDCP layer is to convert the highly redundant headers from upper layers (e.g. IP, UDP, TCP, etc.) into significantly shorter and efficient PDCP packet headers for wireless transport, and vice versa. This header compression step can save precious wireless bandwidth for transporting the data payload.

Typical header compression by ROHC is lossy. Thus, the compressor in ROHC relies on the context of successive packet headers in a single stream (or radio bearer) to remove redundancies. The decompressor also relies on the context for recovering the full IP packet headers upon reception of the compressed headers. The importance of header context at the decompressor means that some decompression failures, which are usually caused by successive packet errors at lower layers, may have serious consequences. When the decompressor loses its context after failing to decompress several packet headers, subsequent PDCP packets could also suffer from decompression failures even if lower layers correctly deliver the packet. Consequently, it is critical to investigate the design trade-off between header compression ratio and robustness against channel errors or packet losses.

C. ROHC Modeling

Consider the system model defined for ROHCv2 [5], in which the ROHC decompressor at the receiver side is modeled as a FSM as shown in Fig. 1. The decompressor maintains a "context" based on which it recovers compressed headers. Such context consists of a static part in the header fields expected to remain unchanged throughout the packet sequence's lifetime (e.g. IP address), plus a dynamically changing part in the header fields (e.g. RTP timestamp) [6, §4.6].

At the start of each packet flow, ROHC decompressor is in "No Context" (NC) state and cannot perform context-based decompression. Hence, ROHC compressor sends Initialization and Refresh (IR) packets with full headers to establish context synchronization between the ROHC compressor and the corresponding decompressor. Upon successfully recovering one of the IR packet headers, the decompressor enters "Full Context" (FC) state, after which packets with fully compressed (CO) headers with a 3-bit cyclic redundancy check (CRC) known as CO_3 headers

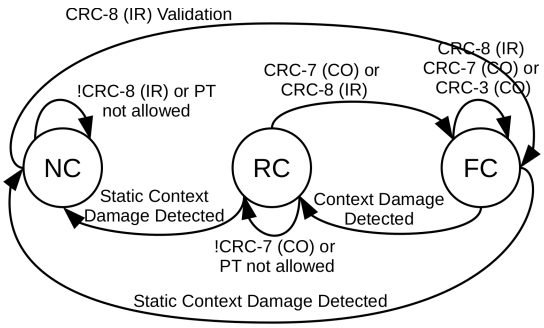

Fig. 1. FSM model of ROHC decompressor (RFC5225).

can be transmitted to allow decompression. Since wireless links between the ROHC compressor and the decompressor are not perfect, decompression failures can occur because of non-ideal conditions such as poor channel quality, noise, and interferences. Repeated header failures can lead to context damage at the decompressor, thereby downgrading the decompressor into lower (RC or NC) states. If context damage is detected in the dynamic header portion, the decompressor would enter the "Repair Context" (RC) state, from which successful decompression of either an IR packet or a weakly-compressed CO packet header with a 7-bit CRC known as CO_7 header with extra context information can repair the dynamic context, allowing the decompressor to transition back and re-enter the FC state. If static context damage is detected in either FC or RC, decompressor will further transition downward to NC, from which only successful recovery of an IR packet header by the decompressor can return its state to FC. Throughout this work, we denote $a_C \in \mathcal{T} = \{0, 1, 2\}$ as IR, CO_7 and CO_3 headers, respectively.

The ROHC compressor at the transmitter does not have direct access to the receiver decompressor state. The ROHC compressor is responsible for controlling the header type of each packet based on its confidence and estimate of its decompressor state. A key header compression algorithm is called the Least Significant Bits (LSB) encoding. In LSB encoding, an interpretation interval of size 2^k is defined for a k-bit encoding scheme such that the header field can be compressed and decompressed so long as its value w.r.t. a reference value (namely the last value transmitted) falls within this interval [5, §5.1.2]. Nevertheless, due to the potential packet loss caused by the channel, the reference value seen by the compressor and the decompressor may not be the same, which would lead to a ROHC decompression failure. In practice, there is a robust version of LSB named Window-based Least Significant Bits (W-LSB) that maintains a sliding window of W reference values instead of a single one. The number of LSBs used to encode a new value is determined as the maximum numbers of LSBs needed w.r.t. each of the W reference values. Consequently, as long as the decompressor's reference value falls within the sliding window, it is in context and is able to decompress the LSB-encoded header field. In other words, a WLSB encoded field can be decoded if there is a consecutive decompression failures of fewer than W packet headers. In practice, the WLSB compression

algorithm may also be limited by the maximum number of LSBs, denoted as k_{max}, that can be used to encode a header field such that a very large header value change cannot be compressed, in which case a packet header without dynamic field compression must be sent.

D. Decompressor Feedback in Bi-Directional ROHC

In the bi-directional mode of operation, the ROHC decompressor sends feedback information to the transmitter to assist the compressor in learning the decompressor state and making compression level decisions. The compressor always starts in uni-directional mode without feedback such that the compressor may rely on periodic resets (by IR packets) to avoid the propagation of context damage. Once a decompressor feedback is received, the compressor will assume that such feedback is always available for this ROHC session [5, §5.2.3] and the compressor may simply rely on this "reliable" feedback channel to better estimate the decompressor state for subsequent header decisions in the bi-directional mode.

Feedbacks provide accurate knowledge on the decompressor's state, based on which the compressor can determine the maximum compression level that can be applied to the header without causing the propagation of context damage, and thus improving the robustness and compression efficiency. However, frequent feedback will also introduce additional cost such as additional bandwidth usage on the reverse-link channel and delays, therefore the ROHC decompressor should limit the rate at which it sends feedback [5, §5.2.3]. Nevertheless, presently it remains unresolved how to address the trade-off between the performance of the ROHC forward channel, namely transmission efficiency and reliability, and the cost on the reverse-link channel from ROHC feedbacks. In this work, we propose a transmitter-initiated feedback polling scheme, in which the compressor at the transmitter directly polls the receiver for decompressor feedbacks according to compressor's need. The polling scheme should be based on the compressor knowledge and confidence on the decompressor's state as well as its design consideration when optimizing the trade-off between the performance and the feedback cost.

E. Channel Model

The Gilbert-Elliot channel model [39] has been a typical framework utilized in existing works [17], [23], [40] on ROHC for modeling the time-varying channels at the ROHC level. The Gilbert-Elliot model characterizes the ROHC channel using a Markov chain consisting of two states: "good" versus "bad". However, the accuracy of such channel model is questionable since most channels' quality may not be easily differentiable as in either "good" or "bad" state. Moreover, the assumption that a packet transmission over the channel always succeeds in "good" state and fails in"bad" state [26] does not fully take into account effective error-control measures such as link-adaptation and HARQ in lower protocol layers. For this reason, as suggested in the original Gilbert-Elliot model [41], a more accurate model with greater granularity to characterize the ROHC channel would be a Markov chain with more states, each associated with a known probability of successful transmission. The parameters of such a channel model can either be estimated [42] or derived from the physical layer channel [43]. Furthermore, owing to the impact of significantly different packet sizes resulting from different levels of header compression, the same lower-layer configuration can still lead to different packet error characteristics for different types of headers.

Similar to our recent work [28], we adopt a general K-state Markov chain with states $\mathcal{K} = \{0,\ 1,\ \cdots,\ K-1\}$ to model the ROHC channel. Such a channel model is characterized by its transition probability from state s_H to $\bar{s}_H$, denoted as $p(\bar{s}_H|s_H)$, $s_H, \bar{s}_H \in \mathcal{K}$, as well as the probability for successful transmission of a packet of type a_C under the channel state $\bar{s}_H$, denoted as $p(\bar{s}_T|a_C,\ \bar{s}_H)$, $a_C \in \mathcal{T}$ and $\bar{s}_H \in \mathcal{K}$, where $\bar{s}_T \in \mathcal{B} = \{0, 1\}$. We use $\bar{s}_T = 0$ and $\bar{s}_T = 1$ to denote failed or successful packet transmission, respectively.

III. A New Trans-Layer Bi-Directional ROHC Compressor Design

To present our novel bi-directional ROHC compressor design based on the trans-layer principle, we first present the assumptions necessary for the Markov model. These assumptions serve to facilitate simple yet meaningful analysis.

A. Assumptions and Notations for State Variables

(A1) The three types of headers and the payload capsule in a packet have fixed lengths, denoted as H_0, H_1, H_2 and L_P, respectively, such that $H_0 > H_1 > H_2$ would reflect different compression levels of IR, CO_7 and CO_3 headers. The total length of IR, CO_7 and CO_3 packets are denoted as L_0, L_1, L_2, respectively, $L_i = H_i + L_P$, $i = 0, 1, 2$.

(A2) The static part of the header remains unchanged throughout the lifetime of the packet sequence (or flow) in question. Hence, only one successful reception of a IR packet is needed for the decompressor to establish the static context.

(A3) The compressibility of the dynamic header part follows a Markov process. Apart from context damage due to consecutive packet losses, if a header is not compressible, an IR or CO_7 header also needs to be transmitted to reinitiate the context.

We have explained our reasoning behind assumptions (A1) and (A2) in our recent work on uni-directional ROHC [28]. For the ROHC system model to be more accurate and practical, we introduce the Markov header source model represented as compressibility in assumption (A3), which is a simplification of [23] based on two considerations: (a) the compressor is typically co-located at the packet source in practice such that it is unnecessary to introduce a channel model between the source and the compressor; (b) the compressibility based on the delta process in [23] depends on probabilities up to the $(W-1)$-th order, leading to a state space whose size grows exponentially with W.

Based on assumptions (A2) and (A3), the ROHC decompressor can be represented by a finite state machine (FSM) in Fig. 2, in which $\text{FC}_\ell,\ \ell = 0,\ \ldots,\ W-1$ denotes that

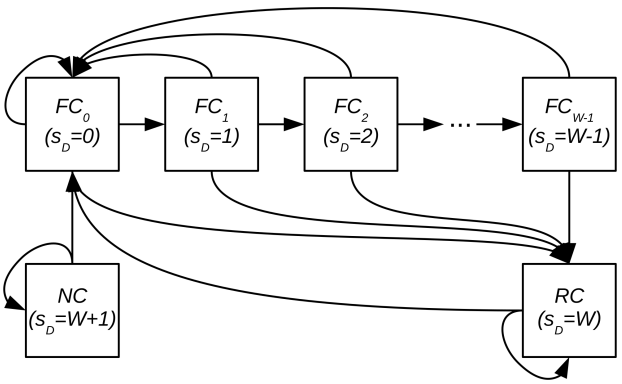

Fig. 2. FSM model of ROHC decompressor for LSB-encoded field.

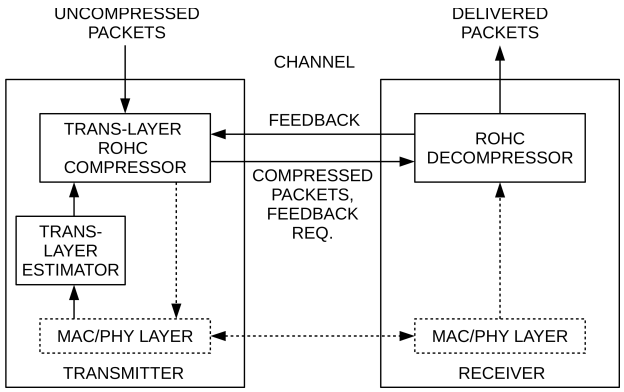

Fig. 3. The system diagram of the trans-layer ROHC design.

the decompressor remains in FC state after losing the last ℓ consecutive packets. Labels NC and RC denote the states as their names suggest. Denote s_S as the state of the header source, where $s_S = 1, 0$ respectively, represents compressible and non-compressible headers. If the decompressor is in FC$_\ell$ state, then we denote $s_D = \ell, \ell = 0, \ldots, W-1$.

For convenience of notation, we let $s_D = W$ and $s_D = W+1$ denote the decompressor state of RC and NC, respectively. Overall, the decompressor's state space is $\mathcal{D} = \{0,\ 1,\ \cdots,\ W+1\}$.

We now define the state transition in Fig. 2, which depends on the header type a_C, the transmission status $\bar{s}_T = \{0,\ 1\}$ and the compressibility $s_S = \{0,\ 1\}$, respectively. Let $\bar{s}_D$ be the next state, then

$$p(\bar{s}_D = W+1 | s_D = W+1) = \mathbf{1}[\bar{s}_T = 0 \vee a_C \neq 0], \tag{1a}$$

$$p(\bar{s}_D = 0 | s_D = W+1) = \mathbf{1}[\bar{s}_T = 1 \wedge a_C = 0], \tag{1b}$$

$$p(\bar{s}_D = 0 | s_D = \ell) = \mathbf{1}[\bar{s}_T = 1 \wedge (s_S = 1 \vee a_C \neq 2)], \quad \ell = 0, \ldots, W-1 \tag{1c}$$

$$p(\bar{s}_D = \ell+1 | s_D = \ell) = \mathbf{1}[\bar{s}_T = 0 \wedge s_S = 1], \quad \ell = 0, \ldots, W-2 \tag{1d}$$

$$p(\bar{s}_D = W | s_D = \ell) = \mathbf{1}[s_S = 0 \wedge (\bar{s}_T = 0 \vee a_C = 2)], \quad \ell = 0, \ldots, W-2 \tag{1e}$$

$$p(\bar{s}_D = W | s_D = W-1) = \mathbf{1}[\bar{s}_T = 0 \vee (s_S = 0 \wedge a_C = 2)], \tag{1f}$$

$$p(\bar{s}_D = W | s_D = W) = \mathbf{1}[\bar{s}_T = 0 \vee a_C = 2], \tag{1g}$$

$$p(\bar{s}_D = 0 | s_D = W) = \mathbf{1}[\bar{s}_T = 1 \wedge a_C \neq 2]. \tag{1h}$$

B. Exploiting Trans-Layer Information

Our investigation on ROHC shall build upon a POMDP framework to exploit trans-layer information as input for controlling compressor decisions. The diagram of our trans-layer design approach is drafted in Fig. 3. In addition to the polled decompressor feedback in bi-directional mode, our ROHC compressor also utilizes the channel state and the transmission status estimation, following the concept first proposed in our previous work on uni-directional ROHC [28].

Continuing our discussion with wireless networks as an example, we note the existence of a plethora of trans-layer information including channel quality information (CQI), hybrid-ARQ (HARQ) feedbacks, frequency of header context initialization, among others. The trans-layer information is complementary to the bi-directional ROHC feedback. Such information is inherent in the network's lower layer activities but has not been designed or envisioned to help derive state information about the ROHC decompressor. Nevertheless, without incurring any additional bandwidth cost, trans-layer information can provide partial information (observation) about the decompressor state.

From the system diagram of Fig. 3, We model the imperfect trans-layer observations as follows:

1) The channel state estimation $z_H \in \mathcal{K}$ is characterized by $p(z_H|\bar{s}_H) = \{\mathbf{E}_H\}_{z_H,\bar{s}_H}$, where $\mathbf{E}_H$ is the channel observation matrix. In other words, the channel manifests as a hidden Markov model (HMM) whose observation space and the state space are identical.
2) The transmission status estimation $z_T \in \mathcal{B}$ is characterized by the transition probability $p(z_T|\bar{s}_T)$ which can be summarily written as $P_{\rm FA}$ and $P_{\rm MD}$, or equivalently in a matrix form

$$\begin{bmatrix} 1-P_{\rm FA} & P_{\rm FA} \\ P_{\rm MD} & 1-P_{\rm MD} \end{bmatrix}.$$

Another practical assumption is that z_T and z_H arrive with a delay of d packet durations.

In contrast, the ROHC feedback $z_D \in \mathcal{D}_b = \{-1, 0, \ldots, W+1\}$ is able to accurately report the decompressor state at the time when the decompressor responds to the polling request from the compressor. In other words, $z_D \in \mathcal{D}_b$ corresponds to the decompressor state defined in Fig. 2. Let $z_D = -1$ denotes no feedback reception. For simplicity and without loss of generality, we further assume that the ROHC feedback is received by the compressor with a delay of d packets, identical to the trans-layer observation delay.

C. A POMDP Formulation

As a powerful tool to address the optimal control problem in a dynamic system that cannot be observed with complete certainty, POMDP is defined by the tuple $\langle \mathcal{S}, \mathcal{A}, \mathcal{Z}, T, O, R \rangle$ [44]: $\mathcal{S}$, $\mathcal{A}$, $\mathcal{Z}$ are the sets of states s, actions a and observations z,

TABLE I
SUMMARY ON POMDP VARIABLES. TYPE 'S', 'A', 'Z' REPRESENTS STATE, ACTION AND OBSERVATION VARIABLES, RESPECTIVELY

Notation	Meaning	Type
$\mathbf{a}_F$	Action history of feedback polling	S
$\mathbf{a}_C$	Action history of header type	S
$\mathbf{s}_S$	State history of header source	S
s_D	Decompressor state	S
s_T	Transmission status	S
s_H	Channel state	S
a_C	Action of header type selection	A
a_F	Action of feedback polling	A
z_D	Delayed observation on decompressor state	Z
z_T	Delayed observation on transmission status	Z
z_H	Delayed observation on channel state	Z

respectively. A transition function $T(s,a,\bar{s}) = p(\bar{s}|s,a)$ denotes the transition probability from s to $\bar{s}$ given $a \in \mathcal{A}$. An observation function $O(\bar{s},a,z) = p(z|\bar{s},a)$ denotes the probability of observing $z \in \mathcal{Z}$ from FSM in state $\bar{s}$ after action a. An instantaneous reward function $R(s,a,\bar{s})$ denotes the immediate reward of transitioning from s to $\bar{s}$ given action a. Generally speaking, the objective of POMDP is to decide the optimal action a at each time slot based on the observation z, in order to maximize the expected long-term reward.

To see how our trans-layer design of bi-directional ROHC can be formulated into a POMDP, the operation of the aforementioned system model is summarized as follows. At time slot t, the ROHC compressor receives channel state and transmission status estimation $z_H[t]$ and $z_T[t]$, as well as the state feedback $z_D[t]$. These three observations serve as *a posteriori* information of the channel state, transmission status, and the decompressor's actual state d time slot ago, due to the observation/feedback delay d. In other words, $z_H[t]$, $z_T[t]$ and $z_D[t]$ are associated with $\bar{s}_H[t-d] = s_H[t-d+1]$, $\bar{s}_T[t-d] = s_T[t-d+1]$ and $\bar{s}_D[t-d] = s_D[t-d+1]$, via the observation functions. The ROHC compressor also keeps track of its belief on $s_H[t-d]$, $s_T[t-d]$ and $s_D[t-d]$, which serve as *a priori* knowledge on $\bar{s}_H[t-d]$, $\bar{s}_T[t-d]$ and $\bar{s}_D[t-d]$ via a state transition function which depends on the header type, the feedback polling, and the header compressibility, denoted as $a_C[t-d]$, $a_F[t-d]$ and $s_S[t-d]$, respectively. By combining *a posteriori* and *a priori* information with Bayesian formula, the belief on the ROHC system's state can be updated. Our POMDP formulation is then completed by associating a reward function, which promotes transmission efficiency and penalizes feedback overhead, with the state of the ROHC system and the action taken.

More specifically, our POMDP-based trans-layer ROHC compressor is illustrated with a dynamic Bayesian network (DBN) in Fig. 4. The variables characterizing the POMDP are summarized in Table I and fully explained as follows:

- The state variables at time slot t, i.e. $\mathbf{s} = (\mathbf{a}_F, \mathbf{a}_C, \mathbf{s}_S, s_D, s_T, s_H) \in \mathcal{S}$, where $\mathbf{s} \in \mathcal{S}$ with state space $\mathcal{S} = \mathcal{B}^{d+1} \times \mathcal{T}^d \times \mathcal{B}^{d+1} \times \mathcal{D} \times \mathcal{B} \times \mathcal{K}$. The 6 components of the state variable at time slot t are defined as:
  1) $\mathbf{a}_F = (a_F[t-1], \ldots, a_F[t-d-1])$ contains the feedback polling history between interval $[t-d-1, t-1]$.
  2) $\mathbf{a}_C = (a_C[t-1], \ldots, a_C[t-d])$, contains the header types transmitted between interval $[t-d, t-1]$.
  3) $\mathbf{s}_S = (s_S[t], \ldots, s_S[t-d])$ denotes whether or not the headers in time interval $[t-d-1, t-1]$ is compressible.
  4) $s_D = s_D[t-d]$ denotes the state of the decompressor at time $t-d$.
  5) $s_T = s_T[t-d]$ denotes the packet transmission status at time $t-d$.
  6) $s_H = s_H[t-d]$ denotes the state of the Markov channel at time $t-d$.

  Note that $\mathbf{a}_F$, $\mathbf{a}_C$ and $\mathbf{s}_S$ are fully observable to the ROHC compressor as it can memorize the actions it had taken and the compressibility of the preceding headers. On the other hand, s_D, s_T and s_H are not fully observable, which reflects the nature of sporadic polled feedbacks and the imperfect trans-layer observation.
- The actions taken by the compressor at time t, i.e. $\mathbf{a} = (a_C, a_F) \in \mathcal{A}$ where $\mathcal{A} = \mathcal{T} \times \mathcal{B}$ denotes the action space. As explained in Sec. III-A, the compressor takes two actions:
  1) $a_C \in \mathcal{T} = \{0,1,2\}$, the header type for the next packet to transmit.
  2) $a_F \in \mathcal{B} = \{1,0\}$, whether to poll a feedback from the decompressor or not.
- The observations by the compressor after its action $\mathbf{a}$ and its state transition to $\bar{\mathbf{s}}$ are $\mathbf{z} = (z_T, z_H, z_D) \in \mathcal{Z}$ where $\mathcal{Z} = \mathcal{B} \times \mathcal{K} \times \mathcal{D}_b$ is the observation space. As explained in Sec. III-B, the observations utilized by the compressor contain three components:
  1) z_T: the transmission status estimation delayed by d.
  2) z_H: the channel state estimation delayed by d.
  3) z_D: the decompressor state feedback delayed by d.

Three functions are defined over these three sets of variables:

- The transition function $T(\mathbf{s},\mathbf{a},\bar{\mathbf{s}}) = p(\bar{\mathbf{s}}|\mathbf{s},\mathbf{a})$ denotes the transition probability from $\mathbf{s}$, the system's state at time t, to $\bar{\mathbf{s}}$, the system's state at time $t+1$, given the action $\mathbf{a} \in \mathcal{A}$:

$$\begin{aligned} T(\mathbf{s},\mathbf{a},\bar{\mathbf{s}}) = {} & p(\bar{\mathbf{s}}_S|\mathbf{s}_S)p(\bar{s}_H|s_H) \\ & \times p(\bar{s}_D|s_D,\bar{s}_T,a_C[t-d],s_S[t-d]) \\ & \times p(\bar{s}_T|a_C[t-d],\bar{s}_H) \\ & \cdot \chi(\mathbf{a}_F,a_F,\bar{\mathbf{a}}_F)\cdot\chi(\mathbf{a}_C,a_C,\bar{\mathbf{a}}_C), \end{aligned} \tag{2}$$

  The state transition function consists of the following conditional probabilities:
  1) The transition of the state history of the header source $\mathbf{s}_S$,

$$\begin{aligned} p(\bar{\mathbf{s}}_S|\mathbf{s}_S) = {} & p(\bar{s}_S[t]|s_S[t]) \\ \mathbf{1}[\bar{s}_S[t-1] = {} & s_S[t] \wedge \ldots \wedge \bar{s}_S[t-d-1] \\ & = s_S[t-d]] \end{aligned} \tag{3}$$

where state transition from $s_S[t]$ to $\bar{s}_S[t] = s_S[t+1]$ follows the Markov header source model defined in Sec. III-A, while the remaining state history needs to be consistent between t and $t+1$.

2) Channel transition probability $p(\bar{s}_H|s_H)$, defined by the Markov model in Sec. II-E.
3) The probability distribution of transmission status, $p(\bar{s}_T|a_C[t-d], \bar{s}_H)$, which depends on the header type and the channel state, and is also defined by the Markov channel model in Sec. II-E.
4) The action history from time t to $t+1$, which is enforced by the indicator function

$$\chi(\mathbf{a}, a, \bar{\mathbf{a}}) = \mathbf{1}[\bar{a}_0 = a \wedge \bar{a}_1 = a_0 \wedge \ldots \wedge \bar{a}_m = a_{m-1}] \quad (4)$$

- The observation function $O(\bar{\mathbf{s}}, \mathbf{a}, \mathbf{z}) = p(\mathbf{z}|\bar{\mathbf{s}}, \mathbf{a})$ denotes the probability of observing $\mathbf{z} \in \mathcal{Z}$ in state $\bar{\mathbf{s}}$ after action $\mathbf{a}$, which is defined as:

$$O(\bar{\mathbf{s}}, \mathbf{a}, \mathbf{z}) = p(z_H|\bar{s}_H)p(z_T|\bar{s}_T) \times \mathbf{1}[(z_D = -1 \ \wedge \ \bar{a}_F[t-d-1] = 0) \vee (z_D = \bar{s}_D \ \wedge \ \bar{a}_F[t-d-1] = 1)], \quad (5)$$

As shown in Sec. III-B, the observation function consists of the following conditional probability functions:

1) $p(z_H|\bar{s}_H)$ that represents the channel estimation function.
2) $p(z_T|\bar{s}_T)$ that represents the transmission status estimation function.
3) The rest of Eq. (5) simply indicating that a state feedback from the decompressor can be received by the compressor at time t if the compressor polls the decompressor at time $t-d-1$.

- The design objective of our POMDP formulation is to maximize the transmission efficiency η penalized with the feedback rate θ. The transmission efficiency is defined as the ratio of the total payload bytes delivered to total bytes transmitted:

$$\eta = \mathbb{E}\left[\frac{\sum_{t=0}^{\infty} L_p \mathbf{1}[s_D[t] = 0]}{\sum_{t=0}^{\infty} L_{a_C[t]}}\right] \quad (6)$$

where $s_D[t] = 0$ represents the event of a successful decompression. The feedback rate θ is defined as the mean feedback request per PDCP packet. Using λ as a trade-off parameter between efficiency and feedback, our goal is to find the optimal policy via

$$\max_{\pi} \eta - \lambda\theta \quad (7)$$

where the policy function π maps observable states and belief on unobservable states to an action, and is to be discussed in detail in Section IV. In order to achieve this objective, the instantaneous reward function $R(\mathbf{s}, \mathbf{a}, \bar{\mathbf{s}})$, which represents the immediate reward gained by moving from $\mathbf{s}$ to $\bar{\mathbf{s}}$ given action $\mathbf{a}$, is designed as follows. To enable a infinite-horizon POMDP formulation, we approximate the transmission efficiency η defined in Eq. (6) with the expected discounted sum of instantaneous transmission efficiency:

$$\tilde{\eta} = \sum_{t=0}^{\infty} \gamma^t \mathbb{E}\left[\frac{L_p \mathbf{1}[s_D[t] = 0]}{L_{a_C[t]}}\right]. \quad (8)$$

where $0 \leq \gamma < 1$ is the discount factor of the infinite POMDP problem. Consequently, our POMDP framework is completed with the definition of reward function:

$$R(\mathbf{s}, \mathbf{a}, \bar{\mathbf{s}}) = L_P/L(a_C[t-d]) \cdot \mathbf{1}[\bar{s}_D = 0] - \lambda \cdot \mathbf{1}[\bar{a}_F[t-d-1] = 1]. \quad (9)$$

where $L(a_C[t-d])$ denotes the total length of packet with header type $a_C[t-d]$.

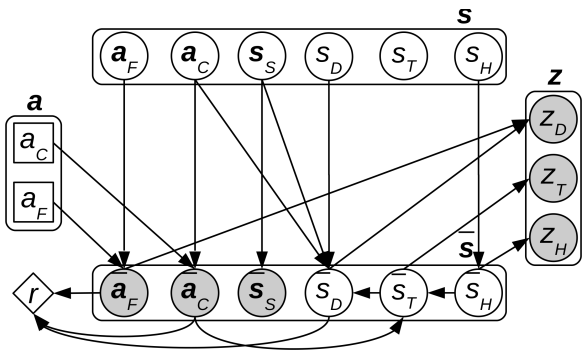

Fig. 4. DBN diagram of POMDP-based bi-directional ROHC.

TABLE II
EXAMPLE 1: A SEQUENCE OF STATE TRANSITIONS, ACTIONS AND OBSERVATIONS FOR $d = 0$

t	s_S	s_D	s_T	s_H	a_C	a_F	z_D	z_T	z_H
0	0	$W+2$	-	π	0	1	-	-	-
1	1	0	1	1	2	0	0	1	1
2	1	1	0	0	2	0	-1	0	0
3	0	0	1	1	2	1	-1	1	1
4	?	$W+1$	1	0	?	?	$W+1$	1	0

It is worth noting that when λ is large enough and the feedback is so heavily penalized that the resulting feedback rate approaches 0, the bi-directional solution effectively degenerates into the uni-directional solution studied in our previous work [28]. On the other hand, when λ is set to 0, the resulting η, when compared with that of the uni-directional solution, represents the maximum performance gain introduced by the feedback. To better illustrate how our trans-layer ROHC system works, we provide two sequences of state transitions, actions, and observations following Fig. 4 as examples with detailed explanations in the next section.

D. Understanding the POMDP Model

A sequence of state transitions, actions and observations based on our trans-layer ROHC design for $d = 0$ is demonstrated in Table II. Note that the state variable $\mathbf{a}_F$ in Fig. 4 has been omitted since it is replaced with the action variable a_F.

- At $t = 0$, the first header to transmit is incompressible ($s_S = 0$) and the decompressor is in NC state

TABLE III
EXAMPLE 2: A SEQUENCE OF STATE TRANSITIONS, ACTIONS AND OBSERVATIONS FOR $d = 2$

t	$\mathbf{a}_C$	$\mathbf{a}_F$	$\mathbf{s}_S$	s_D	s_T	s_H	a_C	a_F	z_D	z_T	z_H
0	$(-,-)$	$(-,-,-)$	$(0,-,-)$	-	-	-	0	1	-	-	-
1	$(0,-)$	$(1,-,-)$	$(1,0,-)$	-	-	-	2	0	-	-	-
2	$(2,0)$	$(0,1,-)$	$(1,1,0)$	$W+2$	-	π	2	0	-	-	-
3	$(2,2)$	$(0,0,1)$	$(0,1,1)$	0	1	1	2	1	0	1	1
4	$(2,2)$	$(1,0,0)$	$(1,0,1)$	1	0	0	?	?	-1	0	0
5	$(?,2)$	$(?,1,0)$	$(?,1,0)$	0	1	1	?	?	-1	1	1
6	$(?,?)$	$(?,?,1)$	$(?,?,1)$	$W+1$	1	0	?	?	$W+1$	1	0

($s_D = W + 2$). The last transmission status is unknown but it will not matter ($s_T = -1$). The initial channel status is also unknown and follows the stationary distribution of the Markov channel model ($s_H = \pi$). The ROHC compressor decides to transmit an IR packet ($a_C = 0$) and to request a feedback ($a_F = 1$) which triggers a state transition.

- At $t = 1$, the channel state corresponding to the first packet transmitted is $s_H = 1$ and the corresponding transmission is successful ($s_T = 1$); Hence the decompressor is now in FC_0 state ($s_D = 0$). The next header to transmit is compressible ($s_S = 1$). Assuming the channel state and transmission status estimate are both correct, we have $z_H = 1$ and $z_T = 1$. Also as a ROHC feedback has been requested at $t = 0$, the decompressor's state is also observed ($z_D = 0$). The ROHC compressor then decides to transmit a CO_3 packet ($a_C = 2$) but requests no feedback ($a_F = 0$).
- At $t = 2$, the channel state corresponding to the second t transmitted packet is $s_H = 0$ and its transmission has failed ($s_T = 0$), sending the decompressor into FC_1 state ($s_D = 1$). The next header to transmit is compressible ($s_S = 1$). Again correct channel state and transmission status estimate lead to $z_H = 0$ and $z_T = 0$. Since no ROHC feedback was polled at $t = 1$, the decompressor state is not observable ($z_D = -1$). The compressor then decides to transmit a CO_3 packet ($a_C = 2$) but requests no feedback ($a_F = 0$).
- At $t = 3$, the channel state corresponding to the third packet transmitted is $s_H = 1$ and its transmission is successful ($s_T = 1$). Thus, the decompressor reverts back to FC_0 state ($s_D = 0$). The next header to transmit is incompressible ($s_S = 0$). The channel state and transmission status are still correctly observed as $z_H = 1$ and $z_T = 1$. Since no ROHC feedback was polled at $t = 2$, the decompressor state is unobservable ($z_D = -1$). The ROHC compressor then decides to transmit a CO_3 packet ($a_C = 2$) and to also request a feedback ($a_F = 1$).
- At $t = 4$, the channel state corresponding to the fourth packet transmitted is $s_H = 0$ and the corresponding transmission is successful ($s_T = 1$). However, since the header scheduled at $t = 3$ is incompressible, given a fully compressed CO_3 header transmission, the decompressor now enters RC state ($s_D = W + 1$). The channel state and transmission status are still correctly observed as $z_H = 0$ and $z_T = 1$. Since a ROHC feedback has been requested at $t = 3$, the decompressor state is observable as $z_D = W + 1$.

Now we consider a second example which experiences the same sequence of channel states, transmission status, header compressibility, ROHC compressor actions and observations. The only difference from the previous example is that now there is an observation delay of $d = 2$ packets. Following the definition in Fig. 4, the state variables are re-defined as:

- $\mathbf{a}_F = (a_F[t-1], \ldots, a_F[t-d-1])$, the feedback request history up to $d+1$ packets ago.
- $\mathbf{a}_C = (a_C[t-1], \ldots, a_C[t-d])$, the header compression type history up to d packets ago.
- $\mathbf{s}_S = (s_S[t], \ldots, s_S[t-d])$, the header compressibility history up to d packets.
- $s_D = s_D[t-d]$, the decompressor state d packets ago.
- $s_T = s_T[t-d]$, the transmission status d packets ago.
- $s_H = s_H[t-d]$, the channel state d packets ago.

The sequence of state transitions, actions, and observations are demonstrated in Table III, which illustrates how state transitions and observations are "shifted", depending on historical actions.

E. POMDP Framework Summary

The sequence of operations of the POMDP framework is as follows: At each time slot t, the ROHC compressor keeps track of the belief $q_t(\mathbf{s}_U)$ on all the unobservable state variables $\mathbf{s}_U = (s_D, s_T, s_H)$. It also maintains the exact state of the observable state variables $\mathbf{s}_O = (\mathbf{a}_F, \mathbf{a}_C, \mathbf{s}_S)$. The POMDP must decide the best action to take according to the solution of its policy by mapping its full state space over $\mathbf{s}_U$ and $\mathbf{s}_S$ to the action space $\mathcal{A}$. In other words, if we let $\mathcal{S}_U$ denote the state space of $\mathbf{s}_U$ and let $\mathbf{q}_U = \{q_t(\mathbf{s}_U) : \mathbf{s}_U \in \mathcal{S}_U\}$ be an $|\mathcal{S}_U|$-dimensional vector containing its current beliefs, then the POMDP decision policy is simply $\mathbf{a} = \hat{\pi}(\mathbf{q}_U, \mathbf{s}_O)$.

Action $\mathbf{a} = \hat{\pi}(\mathbf{q}_U, \mathbf{s}_O)$ at time t will trigger another state transition, leading to new observation $\mathbf{z}$ and $\bar{\mathbf{s}}_O$. The compressor updates its belief over the unobserved states according to [44, §12]:

$$q_{t+1}(\bar{\mathbf{s}}_U) = [p(\mathbf{z}|\mathbf{a})]^{-1} O(\bar{\mathbf{s}}_U, \mathbf{a}, \mathbf{z}|\bar{\mathbf{s}}_O) \times \sum_{\mathbf{s}_U \in \mathcal{S}_U} T(\mathbf{s}_U, \mathbf{a}, \bar{\mathbf{s}}_U|\mathbf{s}_O) q_t(\mathbf{s}_U), \quad \forall \bar{\mathbf{s}}_U \in \mathcal{S}_U \tag{10a}$$

$$p(\mathbf{z}|\mathbf{a}) = \sum_{\boldsymbol{\beta} \in \mathcal{S}_U} O(\boldsymbol{\beta}, \mathbf{a}, \mathbf{z}|\bar{\mathbf{s}}_O) \sum_{\mathbf{s}_U \in \mathcal{S}_U} T(\mathbf{s}_U, \mathbf{a}, \boldsymbol{\beta}|\mathbf{s}_O) q_t(\mathbf{s}_U). \tag{10b}$$

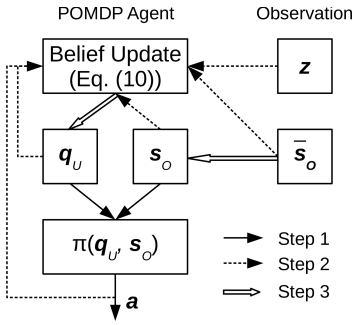

Fig. 5. The diagram of POMDP framework. Step 1: the policy function takes $\mathbf{q}_U$ and $\mathbf{s}_O$ as input to compute the optimal policy $\mathbf{a}$; Step 2: compute the belief on the unobservable states based after taking the action $\mathbf{a}$ and observe $\mathbf{z}$ and $\bar{\mathbf{s}}_O$; Step 3: update the belief on the unobservable variables $\mathbf{q}_U$ and the value of the observable variables $\mathbf{s}_O$.

where

$$T(\mathbf{s}_U, \mathbf{a}, \bar{\mathbf{s}}_U|\mathbf{s}_O) = p(\bar{s}_H|s_H)p(\bar{s}_D|s_D, \bar{s}_T, a_C[t-d], s_S[t-d]) \times p(\bar{s}_T|a_C[t-d], \bar{s}_H) \quad (11a)$$

$$O(\bar{\mathbf{s}}_U, \mathbf{a}, \mathbf{z}|\bar{\mathbf{s}}_O) = O(\bar{\mathbf{s}}, \mathbf{a}, \mathbf{z}), \quad (11b)$$

while $\bar{\mathbf{s}}_O$ are directly observed. From here, the POMDP enters the next stage of $t+1$. The POMDP framework is demonstrated in Fig. 5.

IV. Solving the POMDP Problem and a Complexity Analysis

In general it is difficult to solve POMDP problems exactly due to their high complexity [45]. Nevertheless, there are a number of efficient approximate solutions such as MDP-based heuristics and point-based value iteration methods as mentioned in [44, §12.3] and the references therein. Multiple implementations are available for POMDP problems of various sizes [46]–[49]. In this work, we adopt the SARSOP algorithm [46] for solving POMDP on a general-purpose PC which can provide satisfactory solutions for state space with size in the order of 10^4 within seconds. Since the POMDP problem needs only to be solved once for anticipated channel settings *a priori*, our proposed algorithm can be executed during each user's ROHC negotiation or even offline followed by a simple policy look-up based on the channel setting.

On the other hand, the run-time complexity of the POMDP stems from two types of operations for each packet to transmit. First, the complexity to perform the belief update in Eq. (10) is $O(|\mathcal{S}_U|^2) = O((2K(W+2))^2)$. Second, the complexity to select the optimal action involves evaluating the numerical solution of the policy function $\hat{\pi}(\cdot)$. The optimal value function of the finite-horizon POMDP is piecewise linear and convex (PWLC), while the optimal value function of the discrete infinite-horizon POMDP can be approximated asymptotically by a PWLC function [50], [51]. Specifically, most POMDP algorithms including SARSOP construct their policy function based on a set of mappings, each associated with a possible value of the observable variable $\mathbf{s}_O \in \mathcal{S}_O$. Among them, the mapping associated with the observable variable $\mathbf{s}_O$ is denoted as $\mathcal{V}_{\mathbf{s}_O} \to \mathcal{A}$: $\pi_{\mathbf{s}_O}(\mathbf{v})$, which maps $|\mathcal{S}_U|$-dimensional vector $\mathbf{v} \in \mathcal{V}_{\mathbf{s}_O}$ to an action $\mathbf{a} \in \mathcal{A}$ and $\mathcal{V}_{\mathbf{s}_O}$ is given by the numerical solver. The policy function is evaluated as:

$$\hat{\pi}(\mathbf{q}_U, \mathbf{s}_O) = \pi_{\mathbf{s}_O}\left(\arg\max_{\mathbf{v}\in\mathcal{V}_{\mathbf{s}_O}} \mathbf{v}^T\mathbf{q}_U\right) \quad (12)$$

Hence the maximum complexity to evaluate the policy function once is $\max_{\mathbf{s}_O\in\mathcal{S}_O} O(|\mathcal{V}_{\mathbf{s}_O}||\mathcal{S}_U|)$.

V. Low Complexity Bi-Directional ROHC Compressor Design

In the previous sections, we have rigorously formulated our trans-layer bi-directional ROHC compressor design into a POMDP and provided a complexity analysis for using typical solvers. However the large state space of size $|\mathcal{S}| = 8\cdot 12^d(W+3)K$, which scales exponentially w.r.t. the feedback and the trans-layer estimation delay, makes it difficult to solve the POMDP offline. Furthermore, the PWLC evaluation of the policy function introduced in the last section may lead to high storage requirement and computational complexity at runtime. These shortcomings prompt us to develop suboptimal approaches for additional complexity reduction. In this section, we propose a heuristic policy function that is based on the same belief update process in Eq. (10) with a complexity that scales linearly with the observation delay d.

It is noted that the run-time belief-update does not suffer from the exponentially-growing complexity w.r.t. the delay d, unlike the process for solving the POMDP. Consequently, we propose a sub-optimal policy for the ROHC based on the same belief-update procedure as in Eq. (10). The key idea of this sub-optimal policy is as follows:

- Select the header type a_C by thresholding the probability of the decompressor currently being in NC/RC state and the current header source state.
- Select the feedback action a_F by thresholding the entropy of the marginal distribution of the decompressor's current state.

Both criteria require computing the probability distribution of $s_D[t]$ from the belief of the ROHC system, i.e. the joint probability distribution of $(s_D[t-d], s_T[t-d]. s_H[t-d])$, as well as the header type history and the header source state history from $t-d$ to t. The joint probability distribution can be iteratively evaluated as

$$p(\mathbf{s}_U[t-m+1]) = p(\mathbf{s}_U[t-m])T(\mathbf{s}_U[t-m], a_C[t-m], \mathbf{s}_U[t-m+1]|s_S[t-m]), \quad (13)$$

for $m = 1, \ldots, d$, by noticing that $T(\mathbf{s}_U, \mathbf{a}, \bar{\mathbf{s}}_U|\mathbf{s}_O)$ in Eq. (11) depends on $\mathbf{a}$ and $\mathbf{s}_O$ only via $a_C[t-d]$ and $s_S[t-d]$, respectively. Then the marginal distribution of $s_D[t]$ can be simply evaluated as $p(\mathbf{s}_D[t]) = \sum_{s_T[t]}\sum_{s_H[t]} p(\mathbf{s}_U[t])$. The suboptimal policy for stationary stage ROHC is summarized in Algorithm 1.

This algorithm does not require solving POMDP. Therefore, there is no offline computation complexity. The run-time complexity includes that of the belief update in step-14, which is $O((2K(W+1))^2)$ as discussed in Section IV, as well as that of the "prediction" step to evaluate $p(s_D[t])$ in step-4,

Algorithm 1 Myopic Policy Based on Belief-Update

Select the threshold parameters $P_{D,RC}$, $P_{D,NC}$ and H_D.
Set $t = 0$. Initialize $\mathbf{q}_U[t] = p(\mathbf{s}_U[t-d])$ and $\mathbf{s}_S[t]$.
while Packets being transmitted **do**
  Evaluate $p(\mathbf{s}_U[t])$ with Eq. (13). Then evaluate the entropy $H_U[t]$ of $p(\mathbf{s}_U[t])$.
  if $p(\mathbf{s}_U[t] = W+2) > P_{D,NC}$ **then** $a_C = 0$
  else
    if $s_S[t] = 0$ or $p(\mathbf{s}_U[t] = W+1) > P_{D,RC}$ **then** $a_C = 1$
    else $a_C = 2$
    end if
  end if
  if $H_U[t] > H_D$ **then** $a_F = 1$
  else $a_F = 0$
  end if
  Take action $\mathbf{a} = (a_F, a_C)$ and observe $\mathbf{z}[t]$ and $s_S[t+1]$. Update the belief for $\mathbf{q}_U[t+1]$ and the observable state $\mathbf{s}_O[t+1]$.
  $t \rightarrow t+1$
end while

TABLE IV
THE DEFAULT SIMULATION SETTINGS

WLSB	$W = 5$
Header/Payload	$L_0 = 59$, $L_1 = 15$, $L_2 = 1$, $L_P = 20$, $l_C = 10$
Channel	$l_B = 5$, $\epsilon = 0.1$; $\rho_B = 0.9$, $\rho_G = 0.1$
Delay	$d = 2$
Trans-Layer Info	$P_{\text{FA}} = P_{\text{MD}} = \epsilon_T = 0.1$ $P(z_H = \text{B}\|s'_H = \text{G}) = P(z_H = \text{G}\|s'_H = \text{B})$ $= \epsilon_H = 0.1$
POMDP Compressor	$\gamma = 0.95$ $\lambda = [0.00, 0.001, 0.01, 0.05, 0.1, 0.2, 0.5]$
Myopic Compressor	$P_{D,NC} = 0.3$, $P_{D,RC} = 0.3$ $H_D = [0, 0.1, 0.2, 0.3, 0.4, 0.6, 0.8, 1]\log(W+3)$

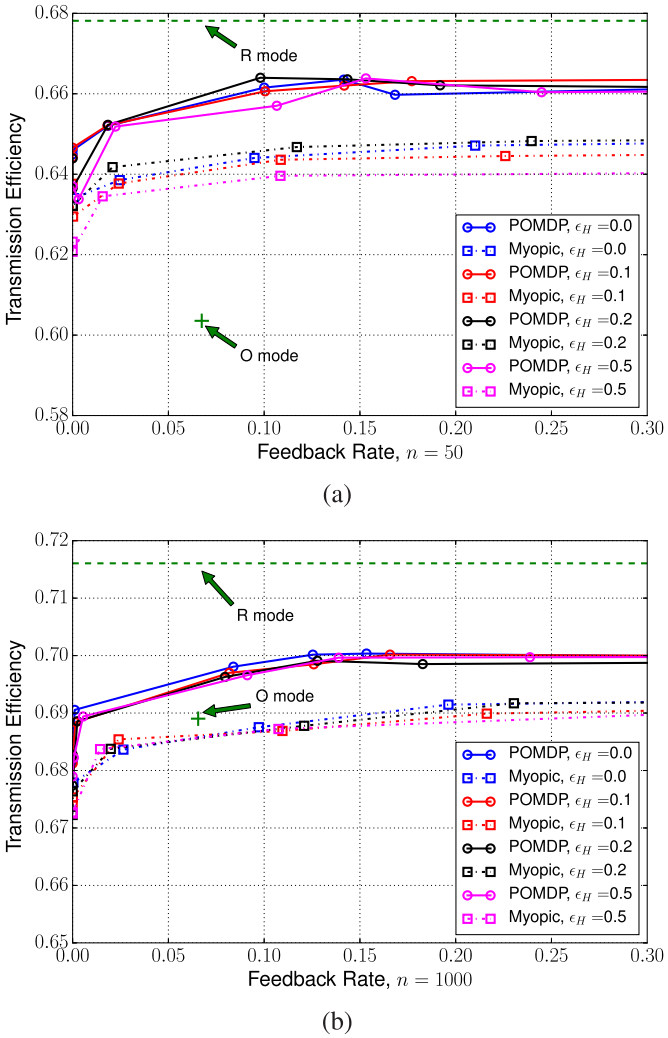

Fig. 6. The empirical efficiency η versus the feedback rate under different channel state estimation error probability ϵ_H.

which is $O(d(2K(W+1))^2)$. Consequently the overall runtime complexity scales well as it only grows linearly with d.

VI. Numerical Examples and Results

In this section we present the numerical results to demonstrate the performance of our proposed trans-layer bi-directional ROHC compressor designs in comparison with the conventional bi-directional ROHC with a practical packet structure, WLSB encoding scheme and Gilbert-Elliot channel model.

A. Test Setup

Unless otherwise noted, we use the following default simulation settings similar to that in our previous work [28] as listed in Table IV.

In addition to the parameters defined in [28], the trade-off between the feedback rate and the transmission efficiency is controlled by the parameter λ and H_D for the POMDP compressor and the myopic compressor, respectively. For each given λ or H_D, a specific policy is determined by solving POMDP in Eq. 7 or given by Algorithm 1, respectively. The resulting empirical (η, θ) are plotted into a trajectory by varying λ or H_D, representing the achievable trade-offs of transmission efficiency and feedback cost by either design approaches. The benchmark comparison is against two conventional bi-directional ROHC compressor designs, namely, the Optimistic mode (O-mode) compressor and Reliable mode (R-mode) compressor.

The O-mode decompressor sends feedback to request context update if it is in NC or RC mode. The R-mode decompressor sends state feedback for each packet and its performance serves as an upper bound of the transmission efficiency. However, in practice it suffers the most from feedback delay and channel idling due to transmission stoppage because the compressor must wait for the feedback from the previous transmission. Let n denote the cumulative number of packets transmitted. All the performance results are compared for two different snap-shots $n = 50$ and $n = 1000$ in the ROHC session in order to characterize both the initial phase and the stationary phase of the header compression operations.

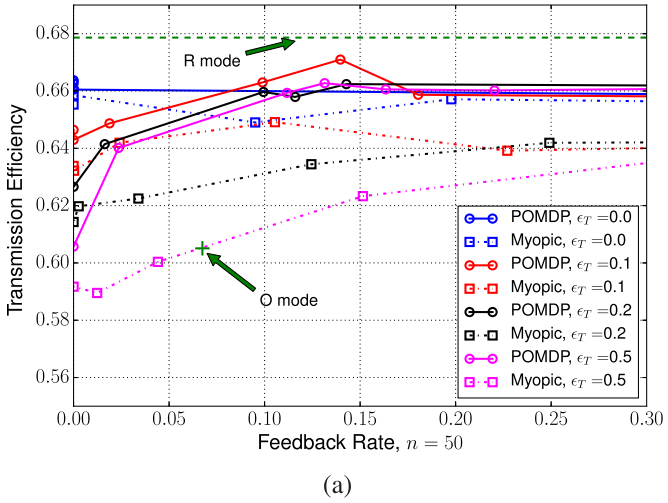

(a)

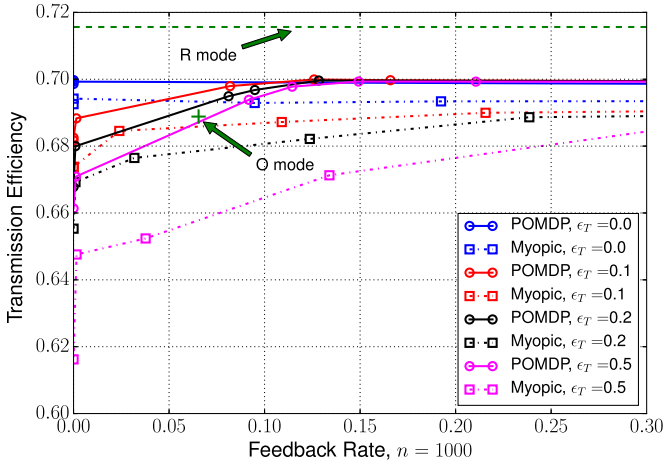

(b)

Fig. 7. The empirical efficiency η versus the feedback rate under different transmission status estimation error probability ϵ_T.

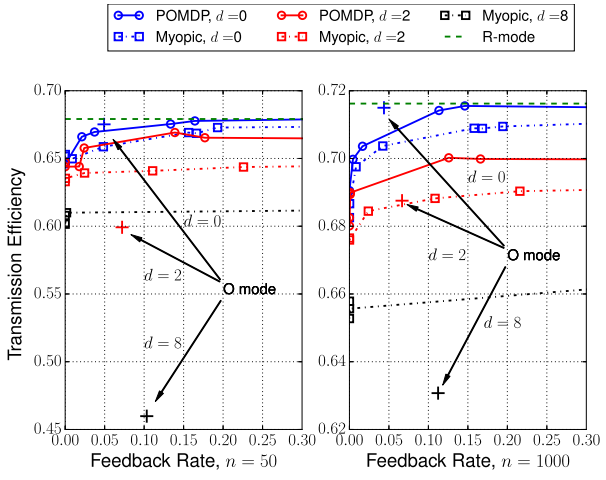

Fig. 8. The empirical efficiency η versus the feedback rate under different feedback/estimation delay d.

All the POMDP instances in our simulation are solved with SARSOP using a timeout setting of 30 seconds, and the resulting maximum gap between the upper and lower bounds of the value function is 5.03%.

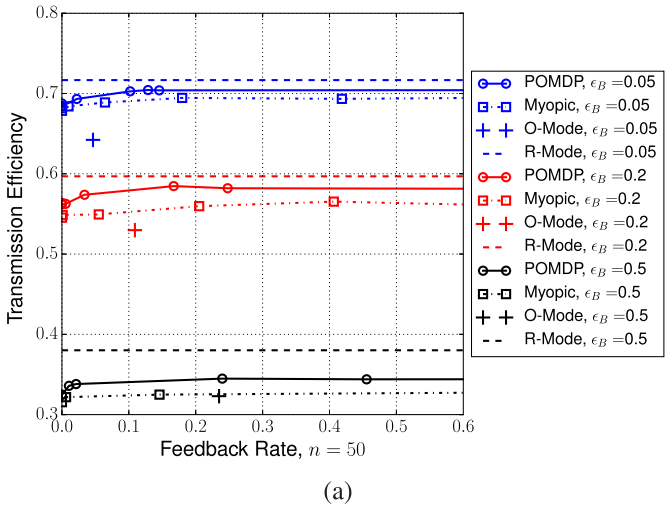

(a)

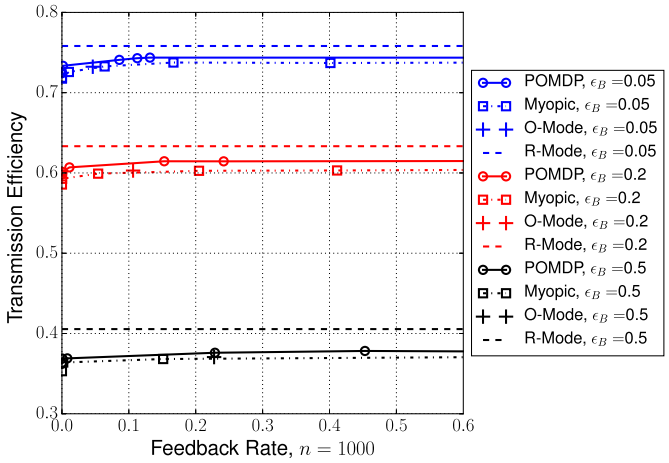

(b)

Fig. 9. η versus the feedback rate under different channel quality ϵ_B.

B. Performance Comparison

In Fig. 6 and Fig. 7, the performance of our two trans-layer compressor designs under different trans-layer information accuracies are compared with that of the two conventional compressors. The accuracies are characterized by the error probability of the channel state estimation, denoted as $p(z_H = B|s'_H = G) = p(z_H = G|s'_H = B) = \epsilon_H$, and that of the transmission status estimation, denoted as $P_{\text{FA}} = P_{\text{MD}} = \epsilon_T$. As we can see, both the POMDP-based compressor and the myopic compressor design achieve higher transmission efficiency over a wide range of feedback rate, particularly during the early stage of the transmission due to the initialization effect. The conventional bi-directional ROHC compressor in comparison shows no performance advantages and cannot support low feedback rate at all.

Note that, similar to our discoveries in previous work [28], the transmission efficiency appears to degrade less gracefully when feedback rate is low for less accurate transmission estimate instead of less accurate channel state estimate. In other words, the trade-off between transmission efficiency and feedback rate is more sensitive to the error in transmission status estimate ϵ_T than that of the channel state estimate ϵ_H.

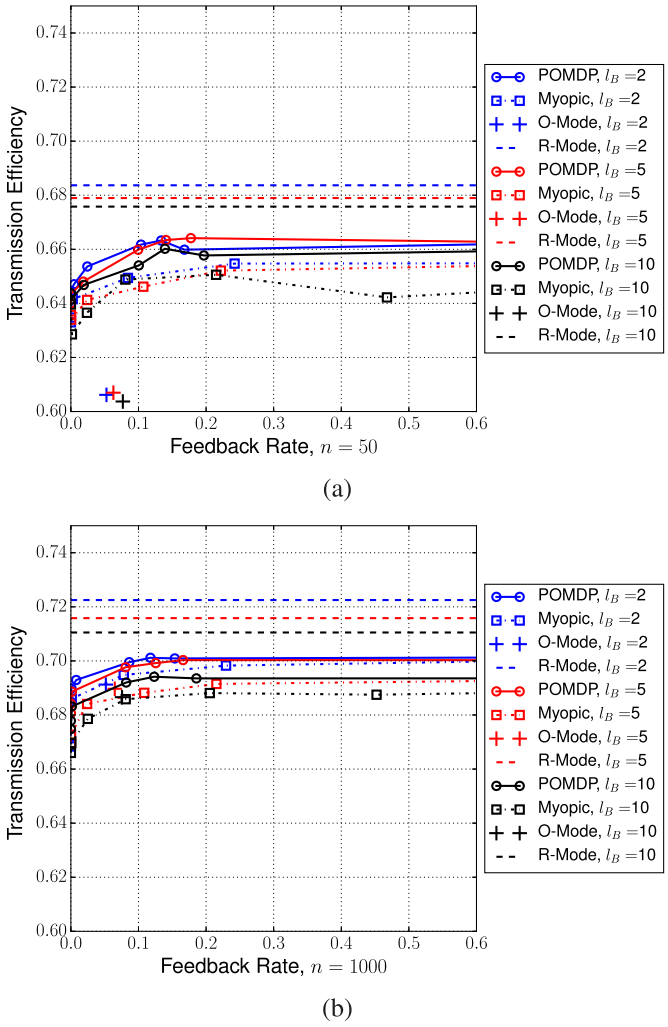

Fig. 10. η versus the feedback rate under different channel coherence l_B.

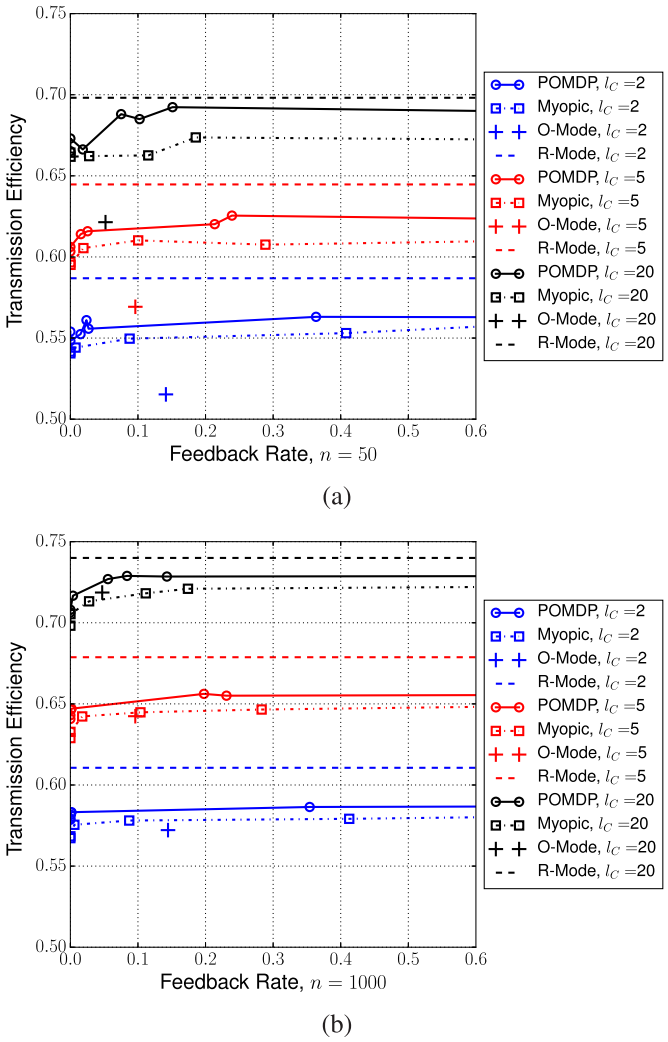

Fig. 11. η versus the feedback rate under different average interval between encountering incompressible headers l_C.

Fig. 8 illustrates the performances of our trans-layer compressor designs under different feedback/observation delays compared against the conventional compressor designs. Note that the transmission efficiency of the R-mode compressor is not affected by the feedback delay d. When there is not feedback delay with $d = 0$, it appears that the O-mode ROHC, in which the decompressor determines when to request a feedback, can achieve a slightly higher transmission efficiency compared to our trans-layer design. Still, its feedback rate requirement is rigid and does not support lower feedback rate at all. As feedback delay d increases, the transmission efficiency of ROHC schemes naturally decreases. We note in particular that the O-mode bi-directional ROHC suffers more severely from the feedback delay than the new trans-layer designs, since the O-mode compressor must wait for the delayed feedback for context repairment. Moreover, its feedback rate increases, suggesting that it requires more frequent context updates. Again this performance gap is particularly noticeable during the initialization phase of a ROHC session.

We further observe the impact of channel qualities on the performances of the ROHC compressors in Fig. 9 and Fig. 10. The Gilbert-Elliot channel is characterized by two variables: the probability of being in the "bad" state ϵ_B and the average duration of consecutive "bad" states l_B. Similar to our previous work [28], ϵ_B and l_B are mapped to state transition probability with $p(\bar{s}_H = \text{G}|s_H = \text{B}) = 1/l_B$, $p(\bar{s}_H = \text{B}|s_H = \text{G}) = p(\bar{s}_H = \text{G}|s_H = \text{B})/(1/\epsilon_B - 1)$. We conclude from these results that the performance of the ROHC compressors relies more heavily on the quality parameter ϵ_B than on the channel coherence parameter l_B. Still, our proposed trans-layer designs allow flexible trade-off between transmission efficiency and feedback rate without suffering much from low feedback rates across all channel settings.

The trade-off between transmission efficiency and the feedback rate under different header source settings is shown in Fig. 11. Let l_C denote the average duration of consecutive compressible headers. In this test, we assume that an incompressible header is always followed by a compressible header, such that $p(\bar{s}_S = 0|s_S = 1) = 1/l_C$, $p(\bar{s}_S = 1|s_S = 0) = 1$. Apparently, when the header source requires more frequent context refreshing, the feedback overhead of the conventional O-mode bi-directional ROHC quickly grows. In contrast, our proposed trans-layer designs

are able to maintain robust transmission efficiency over different feedback rates for various header source settings.

VII. Conclusion

In this work, we investigate the decision optimization with respect to header compression and feedback polling based on a trans-layer framework for bi-directional ROHC systems. Compared to existing O-mode and R-mode bi-directional ROHC compressors, our novel compressor design can benefit from a myriad of trans-layer information readily available from lower layers within typical wireless networks. Our novel ROHC framework improves the transmission efficiency of practical networks, particularly when feedback channel or bandwidth resources are severely limited. Our POMDP framework can optimize trade-offs between transmission efficiency and feedback channel overhead, despite of inaccurate and delayed trans-layer information. To alleviate the high complexity when solving POMDP problems for long feedback/observation delays, we proposed a low-complexity myopic ROHC compressor based on belief update. Compared with traditional compressors, our low-complexity myopic compressor can substantially reduce computational cost with only mild performance loss.

References

[1] Federal Communications Commission. (2010). *Connecting America: The National Broadband Plan*. [Online]. Available: https://www.fcc.gov/general/national-broadband-plan

[2] M. Peng, Y. Li, Z. Zhao, and C. Wang, "System architecture and key technologies for 5G heterogeneous cloud radio access networks," *IEEE Netw.*, vol. 29, no. 2, pp. 6–14, Mar. 2015.

[3] *Evolved Universal Terrestrial Radio Access (E-UTRA); Packet Data Convergence Protocol (PDCP) Specification,* document 3GPP TS 36.323 (v13.2.1), 2016.

[4] C. Bormann *et al.*, *RObust Header Compression (ROHC): Framework and Four Profiles: RTP, UDP, ESP, and Uncompressed*, document RFC 3095, Mar. 2001.

[5] G. Pelletier and K. Sandlund, *RObust Header Compression Version 2 (ROHCv2): Profiles for RTP, UDP, IP, ESP and UDP-Lite*, document RFC 5225, Apr. 2008.

[6] L-E. Jonsson, G. Pelletier, and K. Sandlund, *The RObust Header Compression (ROHC) Framework*, document RFC 5795, Mar. 2010.

[7] EFFNET. (2016). *Effnet Backhaul Compression (BHC)*. [Online]. Available: http://www.effnet.com/products/bhc

[8] Y. Niu, C. Wu, L. Wei, B. Liu, and J. Cai, "Backfill: An efficient header compression scheme for OpenFlow network with satellite links," in *Proc. Int. Conf. Netw. Netw. Appl.*, Jul. 2016, pp. 202–205.

[9] Y. Sun and T. Melodia, "The Internet underwater: An IP-compatible protocol stack for commercial undersea modems," in *Proc. 8th ACM Int. Conf. Underwater Netw. Syst. (WUWNet)*, New York, NY, USA, 2013, Art. no. 37.

[10] E. Demirors, B. G. Shankar, G. E. Santagati, and T. Melodia, "SEANet: A software-defined acoustic networking framework for reconfigurable underwater networking," in *Proc. 10th Int. Conf. Underwater Netw. Syst. (WUWNET)*, New York, NY, USA, 2015, Art. no. 11.

[11] B.-N. Cheng, J. Wheeler, and B. Hung, "Internet protocol header compression technology and its applicability on the tactical edge," *IEEE Commun. Mag.*, vol. 51, no. 10, pp. 58–65, Oct. 2013.

[12] E. J. Hui and P. Thubert, *Compression Format for IPv6 Datagrams Over IEEE 802.15.4-Based Networks*, document RFC 6282, Sep. 2011.

[13] C. Bormann, *6LoWPAN-GHC: Generic Header Compression for IPv6 Over Low-Power Wireless Personal Area Networks (6LoWPANs)*, document RFC 7400, Nov. 2014.

[14] M. Tomoskozi, P. Seeling, P. Ekler, and F. H. P. Fitzek, "Applying robust header compression version 2 for UDP and RTP broadcasting with field constraints," in *Proc. IEEE 85th Veh. Technol. Conf.*, Jun. 2017, pp. 1–5.

[15] M. Tomoskozi, P. Seeling, P. Ekler, and F. H. P. Fitzek, "Efficiency gain for RoHC compressor implementations with dynamic configuration," in *Proc. IEEE 84th Veh. Technol. Conf.*, Sep. 2016, pp. 1–5.

[16] B. Hung, D. Defrancesco, B.-N. Cheng, and P. Sukumar, "An evaluation of IP header compression on the GIG joint IP modem system," in *Proc. IEEE Military Commun. Conf.*, Oct. 2014, pp. 1484–1490.

[17] M. Tömösközi, P. Seeling, and F. H. P. Fitzek, "Performance evaluation and comparison of robust header compression (ROHC) ROHCv1 and ROHCv2 for multimedia delivery," in *Proc. IEEE Globecom Workshops*, Dec. 2013, pp. 544–549.

[18] A. Maeder and A. Felber, "Performance evaluation of ROHC reliable and optimistic mode for voice over LTE," in *Proc. IEEE 77th Veh. Technol. Conf.*, Jun. 2013, pp. 1–5.

[19] E. Piri, J. Pinola, F. Fitzek, and K. Pentikousis, "ROHC and aggregated VoIP over fixed WiMAX: An empirical evaluation," in *Proc. IEEE Symp. Comput. Commun.*, Jul. 2008, pp. 1141–1146.

[20] F. H. P. Fitzek, S. Rein, P. Seeling, and M. Reisslein, "RObust header compression (ROHC) performance for multimedia transmission over 3G/4G wireless networks," *Wireless Pers. Commun.*, vol. 32, no. 1, pp. 23–41, 2005.

[21] A. Minaburo, L. Nuaymi, K. D. Singh, and L. Toutain, "Configuration and analysis of robust header compression in UMTS," in *Proc. IEEE 14th Pers., Indoor Mobile Radio Commun.*, vol. 3, Sep. 2003, pp. 2402–2406.

[22] B. Wang, H. P. Schwefel, K. C. Chua, R. Kutka, and C. Schmidt, "On implementation and improvement of robust header compression in UMTS," in *Proc. IEEE 13th Int. Symp. Pers., Indoor Mobile Radio Commun.*, vol. 3, Sep. 2002, pp. 1151–1155.

[23] C. Y. Cho, W. K. G. Seah, and Y. H. Chew, "A framework and source model for design and evaluation of robust header compression," *Comput. Netw.*, vol. 50, no. 15, pp. 2676–2712, Oct. 2006.

[24] H. Wang and K. G. Seah, "An analytical model for the ROHC RTP profile," in *Proc. IEEE Wireless Commun. Netw. Conf.*, vol. 1, Mar. 2004, pp. 126–131.

[25] S. Kalyanasundaram, V. Ramachandran, and L. M. Collins, "Performance analysis and optimization of the window-based least significant bits encoding technique of ROHC," in *Proc. IEEE Global Telecommun. Conf.*, Nov. 2007, pp. 4681–4686.

[26] R. Hermenier, F. Rossetto, and M. Berioli, "On the behavior of robust header compression u-mode in channels with memory," *IEEE Trans. Wireless Commun.*, vol. 12, no. 8, pp. 3722–3732, Aug. 2013.

[27] P. Barber, "Cross layer design for ROHC and HARQ," IEEE 802.16 Broadband Wireless Access Working Group, 2009. [Online]. Available: http://www.ieee802.org/16/tgm/index.html and http://www.ieee802.org/16/tgm/contrib/C80216m-09_2559r1.doc

[28] W. Wu and Z. Ding, "On efficient packet-switched wireless networking: A Markovian approach to trans-layer design and optimization of ROHC," *IEEE Trans. Wireless Commun.*, vol. 16, no. 7, pp. 4232–4245, Jul. 2017.

[29] A. R. Cassandra, "A survey of POMDP applications," in *Proc. Work. Notes AAAI Fall Symp. Planning Partially Observable Markov Decis. Process.*, vol. 1724, 1998.

[30] G. E. Monahan, "State of the art—A survey of partially observable Markov decision processes: Theory, models, and algorithms," *Manage. Sci.*, vol. 28, no. 1, pp. 1–16, 1982.

[31] M. Hirzallah, W. Afifi, and M. Krunz, "Full-duplex-based rate/mode adaptation strategies for Wi-Fi/LTE-U coexistence: A POMDP approach," *IEEE J. Sel. Areas Commun.*, vol. 35, no. 1, pp. 20–29, Jan. 2017.

[32] J. Seo, Y. Sung, G. Lee, and D. Kim, "Training beam sequence design for millimeter-wave MIMO systems: A POMDP framework," *IEEE Trans. Signal Process.*, vol. 64, no. 5, pp. 1228–1242, Mar. 2016.

[33] J. Wang, C. Jiang, Z. Han, Y. Ren, and L. Hanzo, "Network association strategies for an energy harvesting aided Super-WiFi network relying on measured solar activity," *IEEE J. Sel. Areas Commun.*, vol. 34, no. 12, pp. 3785–3797, Dec. 2016.

[34] S. Padmanabhan, R. G. Stephen, C. R. Murthy, and M. Coupechoux, "Training-based antenna selection for PER minimization: A POMDP approach," *IEEE Trans. Commun.*, vol. 63, no. 9, pp. 3247–3260, Sep. 2015.

[35] M. Abu Alsheikh, D. T. Hoang, D. Niyato, H.-P. Tan, and S. Lin, "Markov decision processes with applications in wireless sensor networks: A survey," *IEEE Commun. Surveys Tuts.*, vol. 17, no. 3, pp. 1239–1267, 4th Quart., 2015.

[36] A. Fanous, Y. E. Sagduyu, and A. Ephremides, "Reliable spectrum sensing and opportunistic access in network-coded communications," *IEEE J. Sel. Topics Signal Process.*, vol. 32, no. 3, pp. 400–410, Mar. 2014.

[37] C. Jiang, W. Wu, and Z. Ding, "LTE multimedia broadcast multicast service provisioning based on robust header compression," in *Proc. IEEE Wireless Commun. Netw. Conf.*, Mar. 2017, pp. 1–6.
[38] C. Jiang, W. Wu, and Z. Ding, "IP packet header compression and user grouping for LTE multimedia broadcast multicast services," in *Proc. Int. Conf. Comput., Netw. Commun.*, Jan. 2017, pp. 52–57.
[39] L. Badia, N. Baldo, M. Levorato, and M. Zorzi, "A Markov framework for error control techniques based on selective retransmission in video transmission over wireless channels," *IEEE J. Sel. Areas Commun.*, vol. 28, no. 3, pp. 488–500, Apr. 2010.
[40] T. K. Madsen, F. H. P. Fitzek, R. Prasad, and M. Katz, "IP header compression for media streaming in wireless networks," in *Proc. IEEE 62nd Veh. Technol. Conf.*, vol. 2, Sep. 2005, pp. 1259–1263.
[41] E. O. Elliott, "Estimates of error rates for codes on burst-noise channels," *Bell Syst. Tech. J.*, vol. 42, no. 5, pp. 1977–1997, Sep. 1963.
[42] G. Hasslinger, A. Schwahn, and F. Hartleb, "2-State (semi-)Markov processes beyond Gilbert-Elliott: Traffic and channel models based on 2^{nd} order statistics," in *Proc. IEEE INFOCOM*, Apr. 2013, pp. 1438–1446.
[43] Q. Zhang and S. A. Kassam, "Finite-state Markov model for Rayleigh fading channels," *IEEE Trans. Commun.*, vol. 47, no. 11, pp. 1688–1692, Nov. 1999.
[44] M. Wiering and M. Van Otterlo, "Reinforcement learning," in *Adaptation, Learning, and Optimization*. Berlin, Germany: Springer, 2012. [Online]. Available: https://link.springer.com/book/10.1007%2F978-3-642-27645-3
[45] W. S. Lee, N. Rong, and D. Hsu, "What makes some POMDP problems easy to approximate?" in *Proc. Adv. Neural Inf. Process. Syst.*, 2007, pp. 689–696.
[46] APPL. *Approximate POMDP Planning Toolkit*. Accessed: Nov. 12, 2018. [Online]. Available: http://bigbird.comp.nus.edu.sg/pmwiki/farm/appl
[47] A. R. Cassandra. *Pomdp-Solve*. Accessed: Nov. 12, 2018. [Online]. Available: http://www.pomdp.org/code/
[48] H. Kurniawati, D. Klimenko, J. M. Song, K. Seiler, and V. Yadav. *APIR: Toolkit for Approximating and Adapting POMDP Solutions In Real Time*. Accessed: Nov. 12, 2018. [Online]. Available: http://robotics.itee.uq.edu.au/~hannakur/dokuwiki/doku.php?id=wiki:tapir
[49] E. Patrick. *POMDPy*. Accessed: Nov. 12, 2018. [Online]. Available: http://pemami4911.github.io/POMDPy
[50] R. D. Smallwood and E. J. Sondik, "The optimal control of partially observable Markov processes over a finite horizon," *Oper. Res.*, vol. 21, no. 5, pp. 1071–1088, 1973.
[51] E. J. Sondik, "The optimal control of partially observable Markov processes over the infinite horizon: Discounted costs," *Oper. Res.*, vol. 26, no. 2, pp. 282–304, 1978.

Wenhao Wu (S'12–M'18) received the B.S. degree in electrical information science and technology from Tsinghua University, Beijing, China, in 2012, and the Ph.D. degree in electrical engineering from the University of California at Davis, Davis, CA, USA, in 2017. Since 2017, he has been a Senior System Engineer at Qualcomm, Inc., San Diego, CA, USA. During his Ph.D. studies, he conducted cooperative research at the Missouri University of Science and Technology, Rolla, MO, USA. His research interests include communications and information theory with special emphasis on multiple-input-multiple-output systems, signal processing for wireless communications, and trans-layer designs.

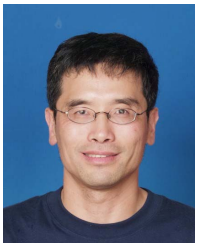

Zhi Ding (S'88–M'90–SM'95–F'03) received the Ph.D. degree in electrical engineering from Cornell University in 1990. From 1990 to 2000, he was a Faculty Member with Auburn University and The University of Iowa. He has held visiting positions at Australian National University, The Hong Kong University of Science and Technology, the NASA Lewis Research Center, and the USAF Wright Laboratory. He is currently a Professor of engineering and entrepreneurship at the University of California at Davis. He actively collaborates with researchers from several countries, including Australia, China, Japan, Canada, Taiwan, South Korea, Singapore, and Hong Kong.

He co-authored *Modern Digital and Analog Communication Systems* (4^{th} edition, Oxford University Press, 2009). He was a member of the Technical Committee on Statistical Signal and Array Processing, and a member of the Technical Committee on Signal Processing for Communications (1994–2003). He has been an active member of the IEEE, serving on technical programs of several workshops and conferences. He received the 2012 IEEE Wireless Communication Recognition Award from the IEEE Communications Society. He was the Technical Program Chair of the 2006 IEEE Globecom. He was an Associate Editor of the IEEE TRANSACTIONS ON SIGNAL PROCESSING (1994–1997 and 2001–2004), and an Associate Editor of the IEEE SIGNAL PROCESSING LETTERS (2002–2005). He has served the IEEE TRANSACTIONS ON WIRELESS COMMUNICATIONS as a Steering Committee Member (2007–2009) and the Chair (2009–2010). He was also an IEEE Distinguished Lecturer [Circuits and Systems Society (2004–2006) and Communications Society (2008–2009)].